

Poor Blade Curvature - A Contributor in the Loss of Performance in the Compressor Unit of Gas Turbine Systems

Chigbo A. Mgbemene

Department of Mechanical Engineering, University of Nigeria, Nsukka 410001

chigbo.mgbemene@gmail.com , +2348034263781

Abstract

The relationship between the curvatures of the blade and the loss of performance of the compressor unit of the gas turbine system was studied. Three blade sets of three different blade curvatures 20°, 35° and 50° were fabricated for this investigation. The blades were tested in a manually fabricated wooden wind tunnel and points of flow separation and vortex height on the trailing edge of each blade set were recorded. The obtained results were then analyzed with respect to the blade velocity distribution effects, compressibility effects and blade loading effects. The analysis indicates that the larger the blade curvature the higher the possibility of poor performance of the system.

Keywords: blade curvature, flow separation, vortex height, velocity, blade loading, stagnation, pressure, suction surface.

1. Introduction

The profile of the gas turbine blades, be it the compressor or turbine blades, has proven to be the most sensitive area of study in the gas turbine plant. Highly expensive brainpower and a lot of man-hours are invested in order to find the blade configurations which will be stable and efficient within specified working angles. Blades must be designed to have correct aerodynamic shape and also be light, tough, and not prone to excessive noise and excessive vibrations. Blades must also be designed to achieve substantial pressure differentials per stage. All these mentioned have direct or indirect relationships to the profile of the blade.

In actual situation, the profile of the compressor and the turbine differ. Higher pressure differentials per stage are achieved in the turbine unit than in the compressor hence fewer stages of turbines are required to drive the compressor unit. The turbine blade profile exhibits deeper curvatures than that of the compressor. This is because the air flow in the compressor is more sensitive to the curvature of the blade profile than it is in the turbine blade profile and if deep curvatures are attempted, the ensuing effects are generally undesirable. Studies have shown that if such curvature is attempted in the compressor blade profile, air flow will tend to separate from the blade surface leading to turbulence, reduced pressure rise, stalling of the compressor with a concurrent loss of engine power and lowered efficiency of the system [1], all which could be termed loss of performance. Theoretically, deeper curvatures should give higher system performance but in the actual situation, loss of performance of the system occurs. For example, stalling of the compressor airfoil blade (which is a loss of performance parameter) results when flow separation occurs over a major portion of the airfoil's suction surface. If the angle of attack of an airfoil is increased, the stagnation point moves back along the pressure surface of the airfoil. The flow on the suction surface then must accelerate sharply to round the nose of the airfoil. The minimum pressure becomes lower, and it moves forward on the suction surface. A severe adverse pressure gradient appears following the point of minimum pressure; finally, it causes the flow to separate completely from the suction surface inducing form drag and the airfoil stalls [2, 3]. A detailed presentation of the review of the studies on stalling and surging of the compressor could be found in Ref. [4].

There are other influences in the system which lead to the poor performance for example, according to Cardamone in Ref. [5] the state of the boundary layer influences, in a major way, the loss development and this loss development directly bears on poor performance of the system.

You and Moin in Ref. [6] presented that flow separation on an airfoil surface is related to the aerodynamic design of the airfoil profile; and that the nature of flow separation on an airfoil is closely related to the performance of the system. From the presentations of Refs. [5, 6] and Hulse et al [7] flow boundary layer separation is related to the

airfoil profile and the performance of the system. Ref. [7] and Bertagnolio et al [8] were able to relate that the blade type affects sound generation by the blade while showing that noise level is also a form of performance measure of the system. They presented that the variations of the separation point along fixed blades, in turn, produce changes in the form of their wake and contribute to the discrete-frequency interaction noise from the rotor.

Indeed, several studies have been carried out on the performance of the axial compressor blade but the studies have concentrated more on the stalling and surging of the axial compressor. But again it has been stated that careful design of compressor blading is necessary to prevent wasteful losses and minimize stalling [9].

To the perception of the author, the effect of the curvature, even to its possible contribution to the stalling and surging of the compressor has not been shown in simple terms for easier understanding. This write-up therefore aims at presenting the relationship between the curvatures of the blade and the loss of performance of the gas turbine system. The effect of the curvature with respect to this loss of system performance was surmised in this paper from the testing of blades with different curvatures. This was done by investigating the relationship between curvatures of the blade with respect to the point of flow separation and vortex height on the trailing edge and subsequently relating them to the velocity distribution effects and blade loading effects due to compressibility effects on the axial type system. This study was carried out by fabrication of model blade cascades at three different blade angles of 20°, 35° and 50°. Each cascade was tested and the results obtained were analyzed. The paper is meant to give the reader a basic idea of the effects of blade curvature in the loss of performance of the gas turbine system.

2. Experimental Approach

2.1 Evaluation of the blade profile

According to Cohen [10] two major requirements of a blade row, whether rotor and stator, are to turn the air through the required angle ($\beta_1 - \beta_2$) in case of the rotor and ($\alpha_2 - \alpha_3$) in the case of the stator; and secondly, carry out diffusing process with optimum efficiency i.e. with minimum loss of stagnation pressure. Consequently, the angle at which the air flows across the blades is critical to the performance of the compressor [11]. One fact remains that air will not leave a blade precisely in the direction indicated by the blade outlet angle, factors like velocity of the air and pressure ratio will affect the exit point. For this reason, to obtain a good performance over a range of operating conditions, it is wise not to make the blade angle equal to the design value of the relative air angle.

According to Cohen [10] the design of blades is much of an art. The design of the blade starts with the sketch of the base profile like as in Fig. 1, from which the blade shape is obtained. The base profile can be constructed or can be determined from the Joukowski transformation of a given circle. It can be defined as the basic shape of an airfoil with a straight camber line (where the camber length equals the chord) as shown in Fig. 2(a) [10].

For subsonic flows, it is necessary to use airfoil section blading to obtain a high efficiency but for increased Mach number flows, blade sections based on parabolas are more effective [10]. For this work, the experiment was carried out in subsonic flow therefore; the base profile with the airfoil shape was used for the blade design. The rotor and stator blades have the same profile and camber arc but are arranged as shown in Fig. 2(b). The base profile generally used for gas turbine blade shape design is the NACA 4-digit series [12]. Details about the design of blades abound in literatures such as in Refs. [10, 12, 13, and 14] but that is not the point of this paper; therefore, this will not be fully discussed.

2.2 The blade design

The ordinates of the base profile t_1 and t_2 are given at definite positions along the camber-line as shown in Fig. 2(a). With the ordinates known the value of the Y_U and Y_L are computed as

$$Y_U, Y_L = \frac{t_n \times l}{100} \quad (1)$$

where t_n = already specified ordinates in Fig. 2(a) as t_1 and t_2

$n = 1$ and 2 for upper and lower sections of the profile respectively

l = camber length (chord).

According to Perkins and Hage [12], in the design of the blade, the centre of the leading edge radius is usually obtained by drawing a line through the end of the chord with slope equal to slope of camber line at 0.5 percent of chord and laying off the leading edge radius along this line. The position of maximum thickness is always 30 percent of the chord [10, 15]. The ratio of maximum thickness and chord (t/c) for blade shapes is generally 10 percent [16]. Following this, the Y values (Y_U and Y_L) were computed and laid off at calculated points on the X axis.

A chord length of 70mm and a blade height of 100mm were chosen for the sake of handling and the size of the wind tunnel that will be used for the testing. A suitable pitch/chord ratio (s/c) of 0.57 (to achieve a high air deflection) [10] and a stagger angle of 34° were chosen. The choices were made based on the actual data from blade samples obtained from gas turbine blades of Afam Power Station Port Harcourt Nigeria which were Asea Brown Boveri gas turbines whose deflection curves agreed with the typical design deflection curve presented in Ref. [10]. Since the blades were to be curved, a circular arc camber line was assumed and the blades were constructed for $\theta = 20^\circ, 35^\circ$ and 50° . The blades operate in cascades with notation as shown in Fig. 3. Figure 4 shows the constructed blades (three sets) which were used for the subsequent tests.

2.3 The low speed wind tunnel (smoke tunnel)

The experiment warranted setting up a special test rig to test the designed blades. A special wind tunnel - an open circuit (or Eiffel) type tunnel was constructed. Because of the size and nature of the experiment, a smoke tunnel was found suitable for the tests [17]. Smoke was introduced ahead of the model being tested. Very low flow speeds were employed for the test to produce a laminar flow into the test section and to avoid the diffusion of the smoke. The wind tunnel was made of wood. It consisted of a smoke pot, a circular duct, rectangular plenum, a rectangular duct with adjustable section (inflow duct), transparent Perspex top, an exit duct, a rectangular chimney and a suction fan. Except the suction fan, every other equipment was locally fabricated with either wood or paper. The arrangement of the wind tunnel is as shown in Fig. 5.

Figure 6 shows front and plan view of the constructed smoke tunnel with a set of blades being tested. The smoke was generated by burning spent engine oil (SAE 40) on embers in a smoke pot and was channeled into the inflow duct through a circular duct. The size of the inflow duct of the tunnel was adjusted such that air (smoke) entered each set of blades at its designed β_l angle. The air (smoke) was drawn in through suction by the fan placed at the end of the chimney. The fan speeds were measured with a Kestrel 3000 digital meter capable of measuring air velocity, temperature, and humidity. Provision was not made for the variation of the spacing between the blades. The observation of the behaviour of air through the blades was visual hence the use of smoke as the fluid medium.

3. Methodology

The tests were carried out with the smoke moving at subsonic speed. Different low speeds were used according to the fan suction speed settings. The speeds were:

- (i) N. speed (NS) – 3.3m/s
- (ii) Speed 1 (S1) – 5.2m/s
- (iii) Speed 2 (S2) – 10.0m/s

Each blade set was placed between the adjustable duct and the exit chimney. The fan (at a given speed) sucked the smoke through the set of blades. The behaviour of the smoke through the set of blades was observed through the Perspex cover. The points of separation from the leading edge of the blade were recorded as well as the height of the vortex formed on the suction surface at the trailing edge. These were done for the three different fan speeds at three different incidence angles (denoted as in Fig 7) and the results recorded. The average values of each set were obtained and were used in the subsequent plot. Although four different sets of plot namely:

- (i) Vortex vs separation graph
- (ii) Variation of angle vs average separation graph
- (iii) Speed vs average separation graph
- (iv) Average vortex vs speed graph (for the 20° @ (-10°) result only)

could be used to describe the results of the experiment, just one set vortex vs separation graph (Fig. 8) is enough for explanations, therefore only that was shown in this paper.

4. Results and Discussions

Separation of flow occurs when the boundary layer has traveled far enough against an adverse pressure gradient such that its energy level drops to a level that the boundary layer speed relative to the object falls almost to zero, the flow then detaches from the object and leaves in form of vortices and eddies. From this study, the point of this separation was found to be affected by, amongst other parameters, the velocity of the flow.

The values of the distance of the points of separation from the leading edge of the blade and the heights of the vortex formed on the suction surface at the trailing edge were recorded and plotted as shown in the Figs. 8 - 10.

Comparing the graphs in sets for the specified angles of 20° , 35° and $50^\circ @ (i = 0^\circ)$; then 20° , 35° and $50^\circ @ (i = +10^\circ)$ and 20° , 35° and $50^\circ @ (i = -10^\circ)$; for the vortex height vs separation point graph (Fig. 8), it could be seen that as the camber angle was decreased or increased, the point at which separation started on the blade decreased or increased respectively. The vortex height also increased or decreased along with the camber angle's increment or decrement respectively. For each angle series for example, $50^\circ @ (i = 0^\circ, +10^\circ \text{ and } -10^\circ)$, it could be observed that a variation in the angle of attack of the air on the blade (Fig.9) affected the behaviour of the air in the blade set. A general trend was observed that as the angle of attack varied from 0° , the point of separation got closer to the leading edge (Fig.10). It was also observed that the negative series (-10°) gave lower separation points but also gave the lowest vortex heights (Figs. 8 and 9), but for the $20^\circ @ (-10^\circ)$ the air separated on hitting the leading edge of the blade resulting in higher vortex than would be expected given the foregoing trend.

A study of the effect of air speed variations with respect to each blade showed that the lower the speed, the higher the separation point or higher the speed, the lower the point of separation.

In the $50^\circ @ (-10^\circ)$, a reversal of trend was noticed; instead of separation point decreasing with increasing speed, it rather increased with increasing speed (Fig. 9a). The separation point despite this reversal was still lower than that of the specified angle $50^\circ @ (0^\circ)$. This may have arisen due to the air hitting the blade at an angle such that the laminar boundary layer separated. According to Cardamone [5] and Anderson et al [18] in the presence of adverse pressure gradients, if the laminar boundary layer separates, transition may take place in a shear layer over the separation bubble. Since a turbulent shear layer has much higher diffusion capability than a laminar one, the flow reattaches usually shortly after transition. This may have been the reason for the trend in the $50^\circ @ (-10^\circ)$.

It was also observed that for any given speed the flow stayed longer on the blade suction surface before separation on the shallower curved blades (Figs. 9 and 10). Vortex heights increased as the speeds were increased leading to turbulent wakes.

Apart from the abnormal behaviour of the air in the $50^\circ @ (-10^\circ)$ blade position, it was observed that generally as the speed was increased the air gradually lost its ability to negotiate curves and then separated from the blade. The degree of separation and formation of vortex depended on the degree of curvature of the blade and also the angle of attack. This effect could be explained by the work of Perkins and Hage in Ref. [12]. They presented that the degree of separation on an aerodynamic body is largely dependent on the magnitude of the unfavourable pressure gradient to the rear of the point of minimum pressure or maximum surface velocity. Therefore, if the pressure gradient, dp/dx , along the surface from this point is equal to or less than zero, then no separation exists. But when the pressure gradient is gradual, the separation occurs so near the rear of the body such that only a very small turbulent wake is produced and the boundary layer is extremely thin everywhere. The drag created by such a body is small and arises mostly from skin friction. If the pressure gradient is high, separation occurs well forward of the rear stagnation point and a turbulent wake exists which alters the potential-flow picture and pressure distribution.

4.1 The consequences of the curvatures

The consequences of a large blade curvature could be seen when the stagnation pressure ratio in a blade row given as Eq. (2) [1] is looked at.

$$\frac{p_{s2}}{p_{s1}} = \left\{ 1 + \frac{(\gamma-1)M_0^2}{1 + \frac{\gamma-1}{2}M_0^2} \frac{\omega}{w_0^2} [(rv)_2 - (rv)_1] \right\}^{\gamma/(\gamma-1)} \quad (2)$$

where p_{s1} and p_{s2} are the stagnation pressures at stations 1 (ahead) and 2 (aft) of the cascade.

From the equation, it could be seen that achieving a large stagnation pressure in the cascade can only be done by having a large curvature but it introduces two deleterious effects – velocity distribution and blade loading effects. A large stagnation pressure will also introduce a large adverse static pressure gradient which leads to boundary layer separation on the blade.

4.1.1 The velocity distribution effect due to the blade curvature

Since the air passing over an airfoil will accelerate to a higher velocity on the convex surface and in a stationary row, this will give rise to a drop in static pressure. This convex surface is termed the suction side of the blade. The concave side will experience a deceleration of the flow and a rise in static pressure hence it is termed the pressure side (Fig 7). Given similar conditions, the velocity distribution through the passage between the pressure side and the suction side will be as presented in Refs. [10, 19] as shown in Fig.11. The maximum velocity on the suction surface will occur at around 10 – 15 percent of the chord from the leading edge after which it falls steadily until the outlet velocity is reached. It was found that relatively thick surface boundary layers resulting in high losses occur in regions where rapid changes of velocity occur, i.e. in regions of high velocity gradient. From Fig. 7, this would most likely occur on the suction surface of the blade. Then increasing the convex nature of the suction surface would increase the velocity gradient further leading to a serious loss due to friction and breakdown of flow with its attendant drop in stagnation pressure.

4.1.2 Blade loading effects

A large blade curvature will lead to a high blade aerodynamic loading and low values of minimum static pressure on the blade suction side [1] and compressibility effects affect the blade loading in that they change the pressure distributions along the blade so that the blade loadings may become excessive. This pressure distribution is related to the permissible deflection in the blade. For a given peripheral speed, the pressure rise obtained in a stage is a function of a coefficient of deflection τ , which for a particular degree of reaction depends on the permissible deflection $\Delta\beta$ of the flow in the cascades [20]. This was shown by Carter [21] and Zweifel [22].

Let us consider the study done by Carter based on observations of an N.G.T.E.[23] profile test data as shown in Fig.12, measured in a 5 in – low speed cascade tunnel of NACA for subsonic flow; here $\theta = \Delta\beta = 18.6^\circ$, the static pressures p on the profile was obtained by means of the pressure coefficients cp . The values of cp at stations (1) and (2) are given as:

$$cp_1 = \frac{P_{s1} - P_1}{(\rho/2)V_1^2} \quad (3)$$

$$cp_2 = \frac{P_{s2} - P_2}{(\rho/2)V_2^2} \quad (4)$$

where p_{s1} and p_{s2} are the total stagnation pressures ahead and aft of the cascade velocities V_1 and V_2 respectively. For an incompressible flow with friction, it is possible to express the frictional losses by the drop of the absolute stagnation pressures at the stations ahead (1) and aft (2) of the cascade. This reduction in absolute stagnation pressure is identical with that of the relative total pressure p_{SR} , since the stream surfaces are coaxial cylinders. The loss through a cascade has also been related to the ideal velocity head which could be produced by a frictionless process between the stagnation pressure p_{s1} and the static pressure p_2 . However, if the velocity diagram Fig.13 [24] is to represent the actual velocities that occur for a process with friction, then the pressure coefficient cp will be given as

$$cp(\xi) = \frac{P_{SR1} - P_{SR2}}{(\rho/2)V_2^2} = \frac{P_{s1} - P_{s2}}{(\rho/2)V_2^2} \quad (5)$$

Neglecting geopotential energy differences, the difference in relative pressures can be given as

$$p_{SR1} - p_{SR2} = p_1 - p_2 + (\rho/2)(V_1^2 - V_2^2) \quad (6)$$

Combining Eqs. (5) and (6) we have

$$p_2 - p_1 = (\rho/2)(V_1^2 - V_2^2) - \xi(\rho/2)V_2^2 \quad (7)$$

The normal force F on the blade can then be represented as

$$F = s\rho V_\infty \Delta V_u - \xi s(\rho/2)V_\infty^2 \frac{\cos^2 \beta_\infty \sin \beta_\infty}{\cos^2 \beta_2} \quad (8)$$

Neglecting the second term we have that

$$F \approx s\rho V_\infty \Delta V_u \quad (9)$$

Introducing the solidity $\sigma = \text{blade chord}/\text{blade spacing}$

$$\sigma = (c/s), \quad (10)$$

and if we express the normal force in terms of the lift coefficient C_L which is dimensionless, then

$$C_L = \frac{F}{(\rho/2)V_\infty^2 c} \quad (11)$$

Combining Eqs. (9) and (11) then

$$C_L = \frac{2\Delta V_u}{\sigma V_\infty} \quad (12)$$

From Fig.13 C_L can then be expressed as

$$C_L = \frac{2}{\sigma} [\tan \beta_1 - \tan \beta_2] \cos \beta_2 \quad (13)$$

From Eq. (13) the link between the permissible deflection and the pressure distribution could be deduced via the lift coefficient. It could also be deduced that the force on the blade depends on the pressure gradient on the suction side of the blade which in turn is affected by the degree of fluid deflection. Therefore, increasing the blade curvature ends up increasing the blade loading.

5. Conclusions

The relationship between the curvatures of the blade and the loss of performance of the gas turbine system has been studied. The discussions have shown that as the curvature was increased from 20° to 50° , the points of separations receded and vortex heights increased and consequently, the detrimental factors that lead to stall and surge in the system were accentuated. Blade aerodynamic loading and the velocity gradient increased with increasing curvature leading to a serious loss due to friction and breakdown of flow with its attendant drop in stagnation pressure. Following these, it can then be concluded that large blade curvature in compressors lead to early flow separations with its adverse effects in the whole compressor system. Therefore, designing blades with large curvatures will lead to loss of performance in the compressor system.

Acknowledgements

The author would like to thank Prof. H. I. Hart of Rivers State University of Technology Port Harcourt and the management of Afam Power Station, Port Harcourt Nigeria for their support towards this project.

References

- [1] Oates, G. C., 1988, *Aerothermodynamics of Gas Turbine and Rocket Propulsion (Revised and Enlarged)*, AIAA Educational Series, American Institute of Aeronautics and Astronautics, Inc., Washington D.C.

- [2] Kay, J. M. and Nedderman, R. M., 1974, *An Introduction to Fluid Mechanics and Heat Transfer*, 3rd Ed., Cambridge University Press, Cambridge, UK.
- [3] Fox, R. W. and McDonald, A. T., 1978, *Introduction to Fluid Mechanics*, 2nd Ed., John Wiley and Sons, New York.
- [4] Mgbemene, C. A., 2002, "The Effect of Blade Curvature in the Failure of Gas Turbine Blades," M.Eng. Thesis, University of Nigeria, Nsukka, Enugu State.
- [5] Cardamone, P., 2006, "Aerodynamic Optimization of Highly Loaded Turbine Cascade Blades for Heavy Duty Gas Turbine Applications," Ph.D Thesis, Universität der Bundeswehr München, Germany.
- [6] You, D. and Moin, P., 2006, "Large-Eddy Simulation of Flow Separation over an Airfoil with Synthetic Jet Control," Center for Turbulence Research Annual Research Briefs, pp 337 – 346, http://ctr.stanford.edu/ResBriefs06/26_You1.pdf, accessed 16 Jan. 2012.
- [7] Hulse, B. T., Lange, J. B., Bateman, D. A. and Change, S.C., 1966, "Some Effects of Blade Characteristics on Compressor Noise Level," FA65WA-1263, Federal Aviation Administration, Washington, D.C.
- [8] Bertagnolio, F., Madsen, H. A. and Bak, C., 2010, "Trailing edge noise model validation and application to airfoil optimization," *Journal of Solar Energy Engineering*, 132, pp 031010-1 - 031010-9.
- [9] Bhushan, N., 2008, "Flow through Centrifugal & Axial Flow Compressors," <http://www.leb.eei.uni-erlangen.de/winterakademie/2008/report/content/course01/pdf/0112.pdf>, accessed 23 Feb. 2012.
- [10] Cohen, H., Rogers, G. F. C. and Saravanamuttoo, H. I. H., 1988, *Gas Turbine Theory*, 3rd Ed., Longman Scientific and Technical, Harlow Essex, UK, Chap. 4.
- [11] Anonymous, 2012, "Fundamentals of Gas Turbine Engines," http://www.cast-safety.org/pdf/3_engine_fundamentals.pdf, accessed 16 Jan. 2012
- [12] Perkins, C. D. and Hage, R. E., 1958, *Airplane Performance Stability and Control*, John Wiley & Sons, Inc., New York, Chap. 2.
- [13] Dixon, S. L., 1998, *Fluid Mechanics and Thermodynamics of Turbomachinery*, 4th Ed., Butterworth-Heinemann, Boston, MA.
- [14] Horlock, J. H., 1958, *Axial Flow Compressors*, Butterworths Scientific Publications, London.
- [15] Carter, A. D. S., Turner, R. C., Sparkes, D. W. and Burrows, R. A., 1960, "The Design and Testing of an Axial-Flow Compressor having Different Blade Profiles in Each Stage," Reports and Memoranda, Ministry of Aviation, Aeronautical Research Council, London, *A.R.C. Technical Report* No. 3183.
- [16] Boyce, Meherwan P., 2002, *Gas Turbine Engineering Handbook*, 2nd Ed., Gulf Professional Publishing, Boston, Chap. 7
- [17] Pope, A. and Harper, J. J., 1966, *Low Speed Wind Tunnel Testing*, John Wiley and Sons Inc., New York.
- [18] Anderson, D. A., Tannehill, J. C. and Pletcher, R. H., 1984, *Computational Fluid Mechanics and Heat Transfer*, Hemisphere Publishing Corporation, New York, NY, pp 374 - 375.
- [19] Elmstrom, M.E., 2004, "Numerical Prediction of the Impact of Non-Uniform Leading Edge Coatings on the Aerodynamic Performance of Compressor Airfoils," Master's Thesis, Naval Postgraduate School, Monterey, CA.
- [20] Sinette, J. T. Jr., Schey, O. W. and King, J. A., 1943, "Performance of NACA Eight Stage Axial Flow Compressor Designed on the Basis of Airfoil Theory," *NACA Report* 758, Washington D.C.
- [21] Carter, A. D. S., 1955, "The Axial Compressor," *Gas Turbine Principles and Practice*, Sir H. R. Cox (Ed.), G. Newnes Ltd, London, Section 5.
- [22] Zweifel, O., 1945, "Optimum Blade Pitch for Turbo-Machines with Special Reference to Blades of Great Curvature," *Brown Boveri Review*, 32.
- [23] Felix, A. R. and Emery, J. C., 1957, "A Comparison of Typical National Gas Turbine Establishment and NACA Axial Flow Compressor Blade Sections in Cascade at Low Speed," *NACA Technical Note* 3937, Washington D.C.
- [24] Vavra, M. H., 1962, *Aero-Thermodynamics and Flow in Turbomachines*, John Wiley & Sons, Inc., New York, NY.

The Figures

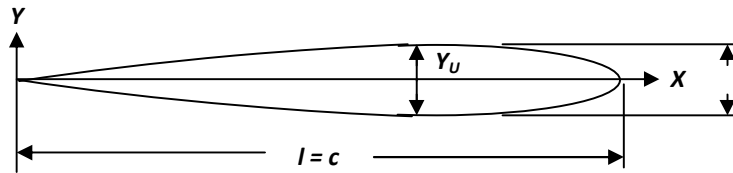


Fig. 1: An aerofoil blade profile.

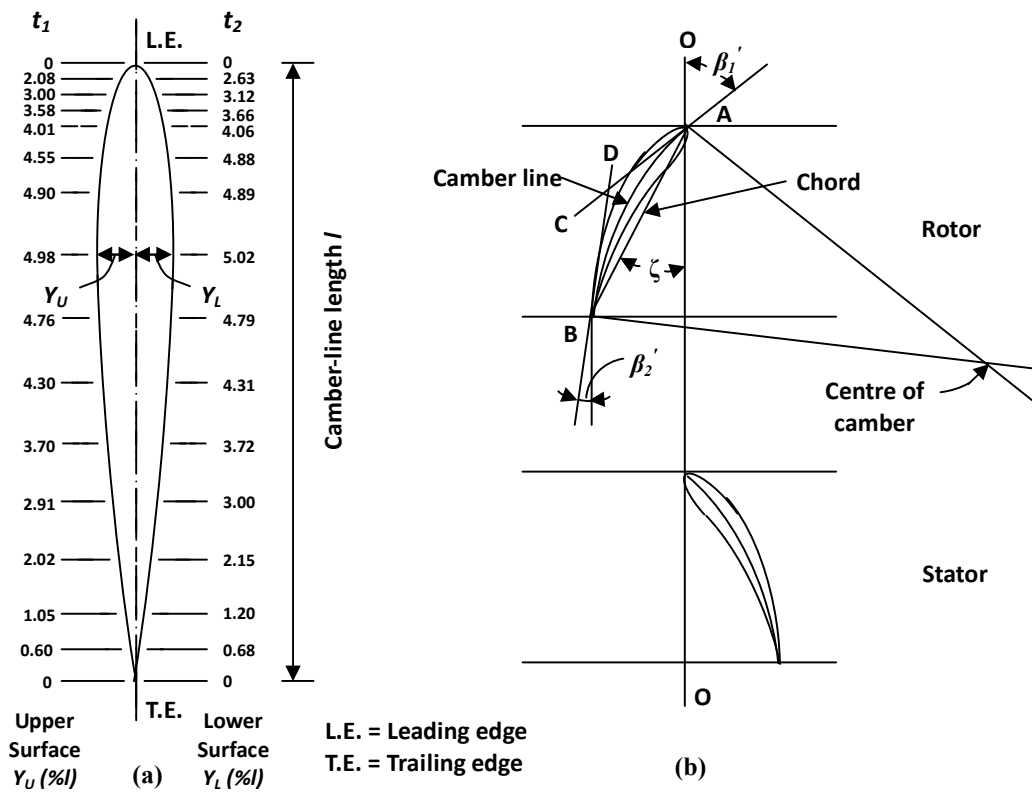


Fig. 2: (a) The blade base profile. (b) The rotor and stator layout in blade design.

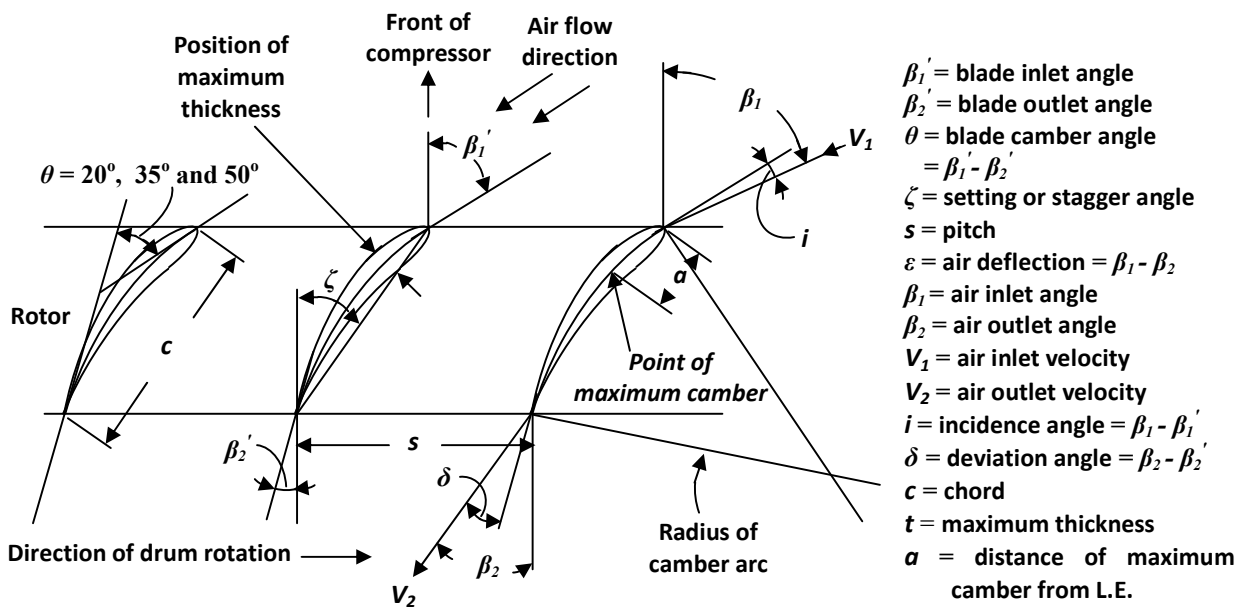


Fig. 3: Compressor cascade and blade notation.

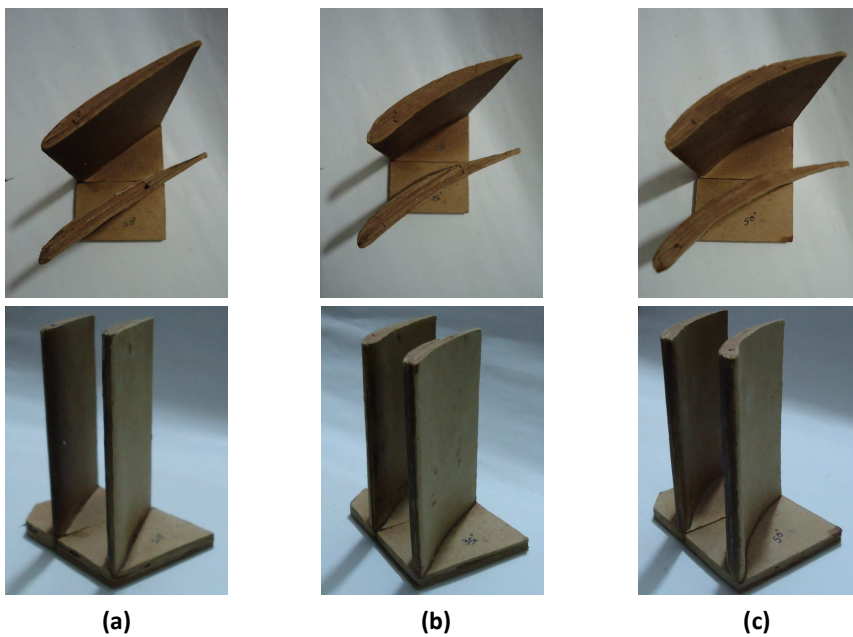


Fig. 4: The fabricated blade samples (a) $\theta = 20^\circ$ (b) $\theta = 35^\circ$ and (c) $\theta = 50^\circ$.

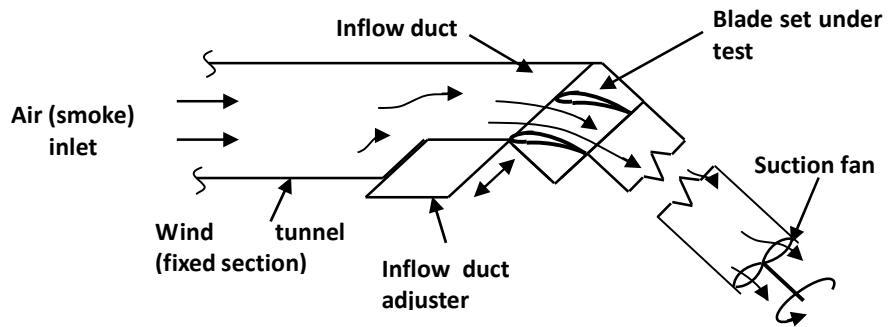


Fig. 5: A schematic diagram of the wind tunnel with a blade set in place.

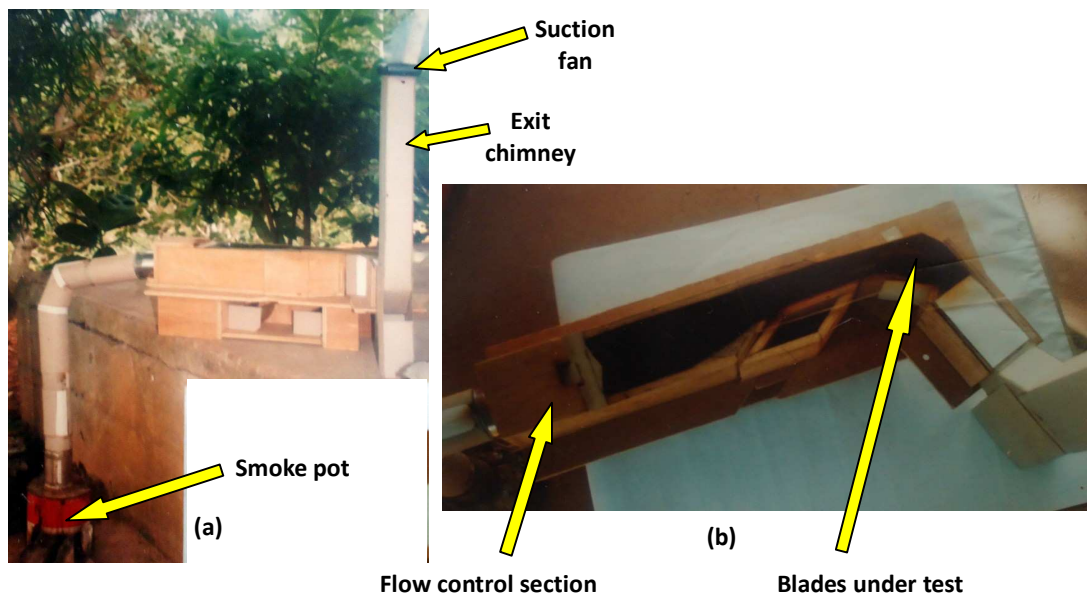


Fig. 6: (a) Front view and (b) Plan view of the wind tunnel.

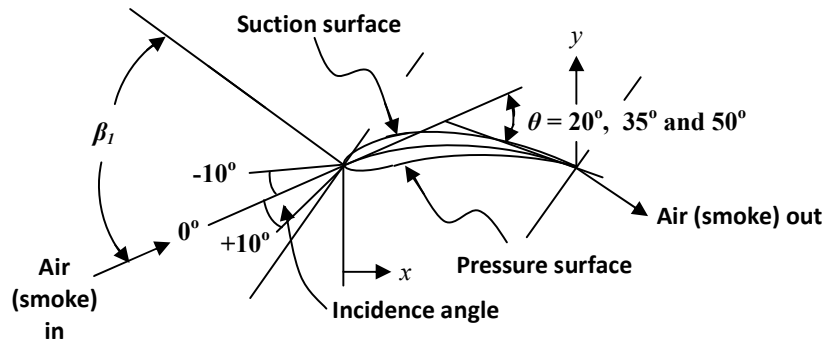


Fig. 7: The blade test nomenclature.

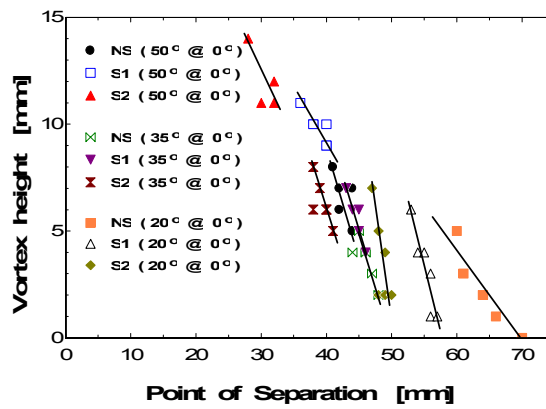


Fig. 8: A plot of Point of Separation against Vortex Height for the (a) $\theta = 20^\circ$, (b) $\theta = 35^\circ$ and (c) $\theta = 50^\circ$ blade sets at $i = 0^\circ$.

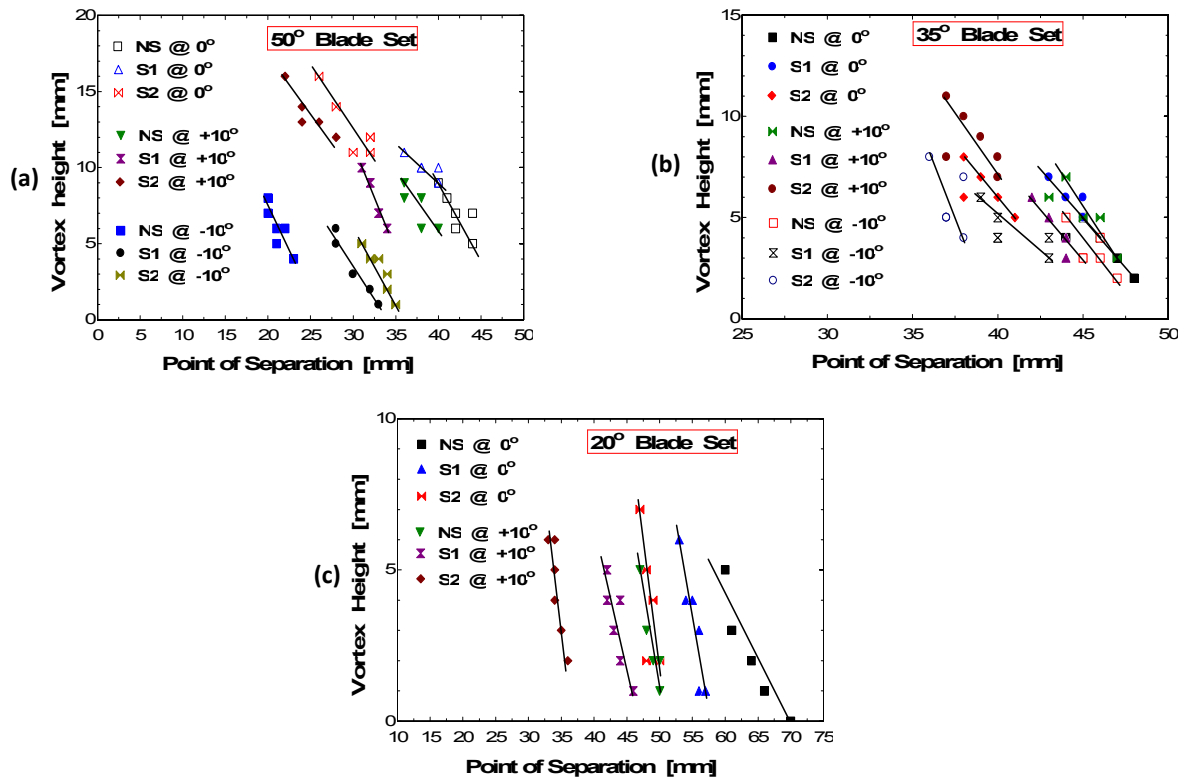


Fig. 9: A plot of Vortex Height vs. Point of Separation.

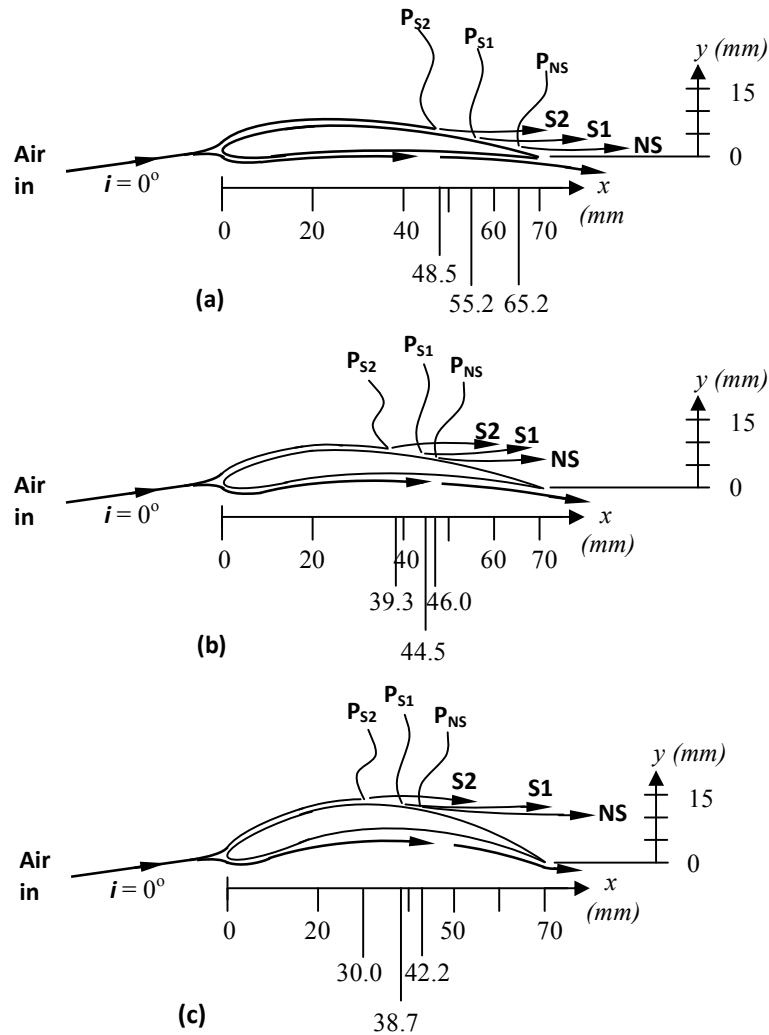


Fig. 10: Points of separation $P_{NS, S1, S2}$ (x axis) and vortex heights (y axis) for the (a) $\theta = 20^\circ$, (b) $\theta = 35^\circ$ and (c) $\theta = 50^\circ$ blade sets.

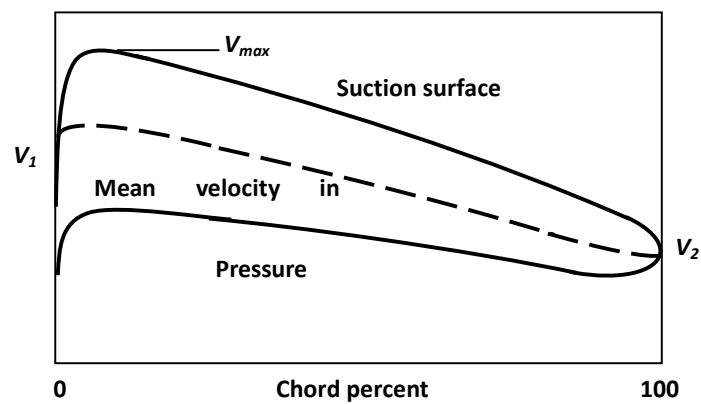


Fig. 11: Typical velocity distribution through the passage of a cascade set [10, 19].

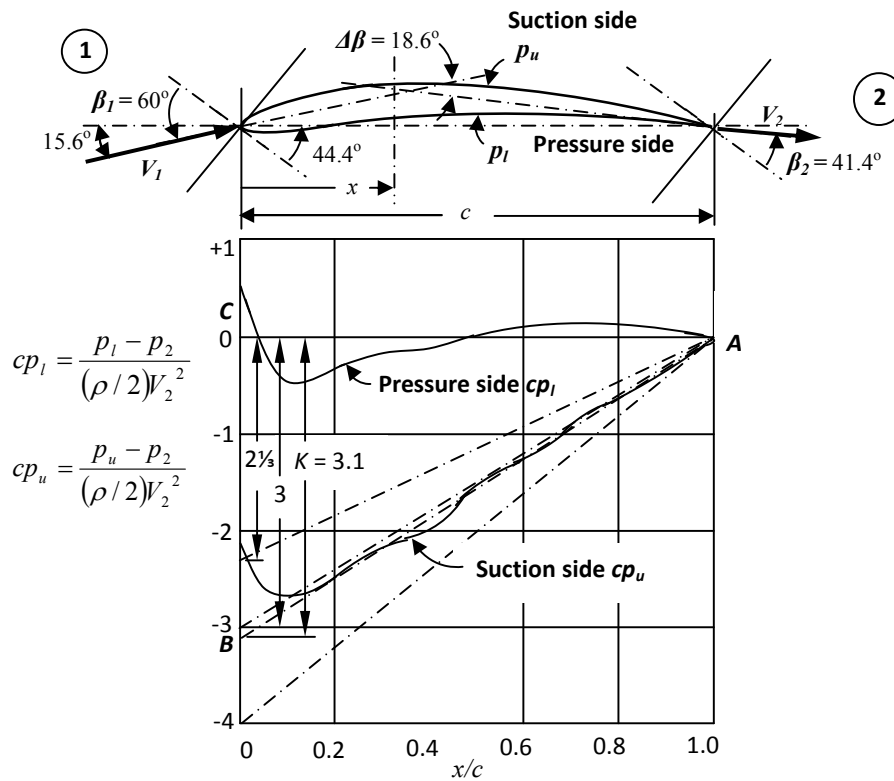


Fig. 12: Measured pressure distribution on profile NGTE 10C4/30C50 in cascade [23].

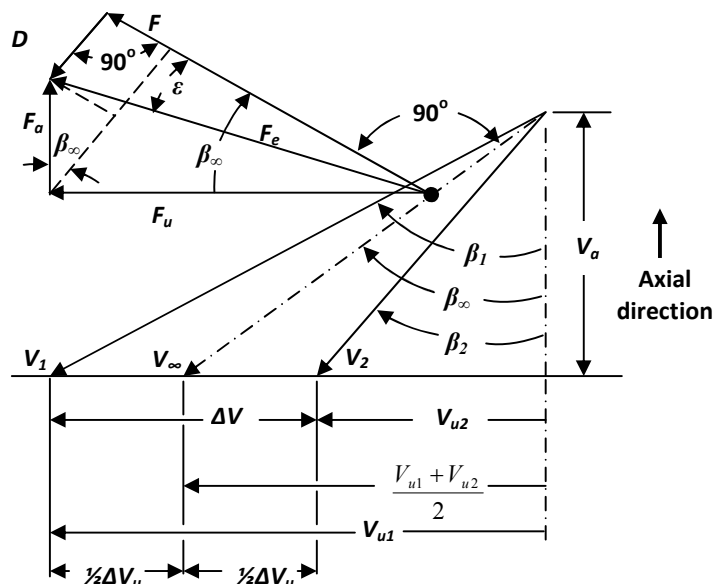


Fig. 13: Velocity diagram of axial flow compressor cascade [24].

This academic article was published by The International Institute for Science, Technology and Education (IISTE). The IISTE is a pioneer in the Open Access Publishing service based in the U.S. and Europe. The aim of the institute is Accelerating Global Knowledge Sharing.

More information about the publisher can be found in the IISTE's homepage:

<http://www.iiste.org>

The IISTE is currently hosting more than 30 peer-reviewed academic journals and collaborating with academic institutions around the world. **Prospective authors of IISTE journals can find the submission instruction on the following page:**

<http://www.iiste.org/Journals/>

The IISTE editorial team promises to review and publish all the qualified submissions in a fast manner. All the journals articles are available online to the readers all over the world without financial, legal, or technical barriers other than those inseparable from gaining access to the internet itself. Printed version of the journals is also available upon request of readers and authors.

IISTE Knowledge Sharing Partners

EBSCO, Index Copernicus, Ulrich's Periodicals Directory, JournalTOCS, PKP Open Archives Harvester, Bielefeld Academic Search Engine, Elektronische Zeitschriftenbibliothek EZB, Open J-Gate, OCLC WorldCat, Universe Digital Library, NewJour, Google Scholar

